Zn^{2+}-Induced Subconductance Events in Cardiac Na^+ Channels Prolonged by Batrachotoxin

Current–Voltage Behavior and Single-Channel Kinetics

LAURENT SCHILD, ARIPPA RAVINDRAN, and EDWARD MOCZYDLOWSKI

From the Department of Pharmacology and the Department of Cellular and Molecular Physiology, Yale University School of Medicine, New Haven, Connecticut 06510

ABSTRACT The mechanism of voltage-dependent substate production by external Zn^{2+} in batrachotoxin-modified Na^+ channels from canine heart was investigated by analysis of the current–voltage behavior and single-channel kinetics of substate events. At the single-channel level the addition of external Zn^{2+} results in an increasing frequency of substate events with a mean duration of ~15–25 ms for the substate dwell time observed in the range of −70 to +70 mV. Under conditions of symmetrical 0.2 M NaCl, the open state of cardiac Na^+ channels displays ohmic current–voltage behavior in the range of −90 to +100 mV, with a slope conductance of 21 pS. In contrast, the Zn^{2+}-induced substate exhibits significant outward rectification with a slope conductance of 3.1 pS in the range of −100 to −50 mV and 5.1 pS in the range of +50 to +100 mV. Analysis of dwell-time histograms of substate events as a function of Zn^{2+} concentration and voltage led to the consideration of two types of models that may explain this behavior. Using a simple one-site blocking model, the apparent association rate for Zn^{2+} binding is more strongly voltage dependent (decreasing *e*-fold per +60 mV) than the Zn^{2+} dissociation rate (increasing *e*-fold per +420 mV). However, this simple blocking model cannot account for the dependence of the apparent dissociation rate on Zn^{2+} concentration. To explain this result, a four-state kinetic scheme involving a Zn^{2+}-induced conformational change from a high conductance conformation to a substate conformation is proposed. This model, similar to one introduced by Pietrobon et al. (1989. *J. Gen. Physiol.* 94:1–24) for H^+-induced substate behavior in L-type Ca^{2+} channels, is able to simulate the kinetic and equilibrium behavior of the primary Zn^{2+}-induced

Address reprint requests to Dr. Edward Moczydlowski, Department of Pharmacology, Yale University School of Medicine, 333 Cedar St., New Haven, CT 06510.

Dr. Schild's present address is Institut de Pharmacologie, de l'Universite de Lausanne, rue du Bugnon 27, CH-1005, Lausanne, Switzerland. Dr. Ravindran's present address is Department of Neuroscience, Johns Hopkins University School of Medicine, Baltimore, MD 21205.

J. GEN. PHYSIOL. © The Rockefeller University Press · 0022-1295/91/01/0117/26 $2.00
Volume 97 January 1991 117–142

substate process in heart Na^+ channels. This model implies that binding of Zn^{2+} greatly enhances conversion of the open, ohmic channel to a low conductance conformation with an asymmetric energy profile for Na^+ permeation.

INTRODUCTION

Subtypes of voltage-dependent Na^+ channels differ in their relative sensitivity to guanidinium toxins such as tetrodotoxin (TTX) and to certain divalent cations. For example, previous studies have shown that TTX-insensitive Na^+ channels are ~50–100-fold more sensitive to inhibition by external Zn^{2+} than TTX-sensitive Na^+ channel subtypes (Frelin et al., 1986; Baumgarten and Fozzard, 1989; Ravindran et al., 1991). In the preceding paper we showed that the inhibitory effect of external Zn^{2+} on TTX-insensitive, cardiac Na^+ channels modified by batrachotoxin (BTX) can be resolved as brief interruptions in the open-channel current (Ravindran et al., 1991). Superficially, this effect of Zn^{2+} resembles a discrete, voltage-dependent block. However, the resolved interruptions induced by Zn^{2+} dwell at a distinct substate level instead of closing to the zero current level defined by closures of channel gating. This latter observation is in conflict with classic models of voltage-dependent block of Na^+ channels by external divalent cations (Woodhull, 1973; Yamamoto et al., 1984), where Ca^{2+} or a similar inorganic ion occupies a specific binding site in the narrow permeation pathway and completely occludes or blocks the passage of Na^+. Rather than complete occlusion, the subconductance block induced by Zn^{2+} resembles the effect of protons or deuterium ions on monovalent ion current through L-type Ca^{2+} channels, where similar subconductance events are induced by lowering external pH or pD (Prod'hom et al., 1987; Pietrobon et al., 1989).

In this paper we document the current–voltage behavior of the Zn^{2+}-induced substate and show that the substate exhibits significant outward rectification in the presence of symmetrical NaCl. In contrast, the open state of the cardiac Na^+ channel displays nearly ohmic current–voltage behavior under the same conditions. We also present a stochastic analysis of fluctuations of single Na^+ channels in the presence of Zn^{2+}. This analysis leads us to consider a kinetic model for Zn^{2+} action similar to one previously proposed for substate block of L-type Ca^{2+} channels by protons (Pietrobon et al., 1989). In this model, binding of Zn^{2+} to a distinct site outside of the permeation path induces a conformational change that results in an asymmetric energy profile for permeation through the channel and a lower unitary conductance for Na^+. However, in contrast to the reported effect of protons on the Ca^{2+} channel, the binding of Zn^{2+} to the heart Na^+ channel is voltage dependent. Parts of this work have been presented in abstract form (Ravindran and Moczydlowski, 1988; Schild et al., 1990).

METHODS

Planar Bilayer Recording and Na^+ Channel Incorporation

Plasma membrane vesicles from canine heart ventricular muscle were used for Na^+ channel incorporation into planar bilayers as described previously (Guo et al., 1987; Ravindran et al., 1991). Single Na^+ channels were studied in neutral phospholipid bilayers (8PE:2PC, 25 mg/ml in decane) under symmetrical buffer conditions: 10 mM MOPS-NaOH, pH 7.4, 0.2 M NaCl at

21–24°C. Voltages are referred to the physiological convention that positive is depolarizing. In the course of these experiments different recording systems were used to collect single-channel data as described in the preceding paper (Ravindran et al., 1991). Lowest noise and superior resolution of the Zn^{2+}-induced substate events was obtained with a List EPC7 amplifier (Medical Systems Corp., Great Neck, NY).

Measurements of Unitary Currents and Dwell Times

The analysis of discrete Zn^{2+}-blocking events described in this paper was based on data collected from 18 single-channel membranes. A given experiment involved steady-state recording of 1–5 min of continuous data taken at different Zn^{2+} concentrations (0–640 μM) and different voltages (primarily ±50, ±60, and ±70 mV) for single-channel membranes that typically last for 1–2 h. The data set includes dwell-time histograms compiled from ~180 records at various voltage and $[Zn^{2+}]$ conditions.

Construction of current–voltage curves for the open-state and Zn^{2+}-induced substate was performed by computer-aided measurements of peak currents from amplitude histograms. Amplitude histograms such as those in Fig. 4 were compiled from 3 s of a single-channel record filtered at 50 Hz and digitized at 2 kHz using an LSI 1173 computer system (Indec Systems, Sunnyvale, CA). Histograms were plotted on a Hewlett-Packard 1345A digital display at a resolution of 5 pA/2,048 bins with arbitrary scaling of the ordinate (number of points). Peak positions of amplitude histograms were marked by eye with a movable on-screen cursor. Current amplitudes were also measured directly from monitor displays of enlarged current records using an Atari computer system with a mouse-driven cursor (Instrutech Corp., Elmont, NY). Both methods gave similar results.

Dwell-time histograms were compiled from 1–2 min of a single-channel record filtered at 200 Hz (−3 db corner frequency, 8-pole lowpass Bessel filter) and digitized at a sampling rate of 2 kHz. For some experiments with higher baseline noise, analysis at 100 Hz filtering was carried out with comparable results. The time resolution of the system is restricted to a dead time, T_d, for the shortest resolvable opening or closing event as estimated from the formula $T_d = 0.179/f_c$, where f_c is the corner frequency (Colquhoun and Sigworth, 1983). The dead time is thus estimated to be ~1 ms at 200 Hz and 2 ms at 100 Hz.

Construction and fitting of frequency density histograms of open and closed dwell times followed the method of Sigworth and Sine (1987), which uses a log-time binning procedure. The histogram representations shown in Figs. 6 and 9 use a square root ordinate with a log-binned time abscissa (10 bins/decade). Dr. Stephen Sine and Dr. Fred Sigworth (Department of Cellular and Molecular Physiology, Yale Medical School, New Haven, CT) kindly supplied the histogram fitting routines for use on an Indec Systems LSI 1173 computer. Similar programs for an Atari computer system were obtained through Instrutech Corp.

Dwell-time analysis of Zn^{2+}-induced substate events in planar bilayers poses technical problems due to the relatively large dead time for the shortest detectable events and kinetic contamination by brief Na^+ channel closing events that occur in the same time range as the substate events. In addition, the current amplitude of the substate is only 0.2 pA above the zero current closed state at −70 mV, which is actually less than the peak-to-peak noise at 100 Hz filtering. Thus, it is not possible to use a simple automatic threshhold criterion to reliably distinguish substate closures from complete closures without compromising time resolution.

Given these circumstances, we developed a strategy that allowed us to identify relatively pure (>90%) populations of substate events with accurately measured durations. This procedure utilized a threshold for event detection that was set at 50% of the current level between the open state and the substate. All events above this threshold were collected into open-state histograms and all events below this threshold were collected into closed-state histograms. The open-state histograms were well fit by a single exponential distribution in the absence and

presence of Zn^{2+}, but the closed-state histograms, containing both complete closures due to gating and substate closures, required at least two exponentials in the absence and presence of Zn^{2+}.

Errors Affecting the Interpretation of Dwell-Time Distributions

In the absence of Zn^{2+} the BTX-modified Na^+ channel from canine heart is steeply activated by voltage in the range of −120 to −80 mV and exhibits a voltage-independent probability of opening of ~0.9 at voltages more positive that −60 mV. This behavior is quite similar to that previously described for BTX-modified Na^+ channels from other tissues studied under similar conditions (Moczydlowski et al., 1984*a*; Keller et al., 1986; Behrens et al., 1989). In this paper we analyzed the Zn^{2+}-induced substate kinetics in the range of −70 to +70 mV in order to focus on the interaction of Zn^{2+} with the open state of the channel and to initially avoid the difficulty of distinguishing the voltage dependence of Zn^{2+} binding from the voltage dependence of channel gating.

At 200-Hz filtering we are able to accurately fit dwell-time constants that are greater than or equal to 10 ms. For example, Fig. 6 *D* shows a fit to an open-state population that has a time constant of 10.3 ms. However, it should be emphasized that such distributions are distributions of apparent openings or apparent closings that are artificially extended due to the effect of respectively missing brief closures or brief openings that are too short to be captured by the 50% threshold criterion (Colquhoun and Sigworth, 1983). Various workers have proposed corrections of such apparent lifetimes to obtain true lifetimes based on explicit derivations or numerical simulations (Colquhoun and Sigworth, 1983; Roux and Sauvé, 1985; Blatz and Magleby, 1986; Milne et al., 1989; Pietrobon et al., 1989). These methods assume that the observed dwell-time distribution can be interpreted within the framework of a particular scheme of closed and open states, with the simplest case being a single closed and single open state in equilibrium. The direct application of such methods to the Zn^{2+}-induced substate behavior is not a straightforward procedure because there are multiple components in the closed state distribution in the absence and presence of Zn^{2+}. In the presence of Zn^{2+} there are also multiple current levels that include fully and partially closed states with transitions between these levels. Since the open-state dwell times are generally well resolved and exhibit a single exponential distribution, it is possible to apply a small correction for missed events in this case. However, given the complexity of the closed-state/substate behavior, we do not feel that it is appropriate to assume a particular scheme and apply dwell-time corrections based on one model. Instead, we present the actual uncorrected histograms of observed events and evaluate possible errors that could lead to misinterpretation. Despite the uncertainties inherent in this approach, we were able to accurately reconstruct the equilibrium behavior of Zn^{2+} titrations solely from kinetic parameters derived from dwell-time histograms. This gives us confidence that our methods provide a reasonable approximation to the kinetics of the substate process.

The mean dwell time of the single-exponential open state was observed to continuously shorten with increasing concentrations of external Zn^{2+} (e.g., Figs. 2, 3, and 6). We wished to avoid missing > 10% of real opening events, because missed openings artificially lengthen dwell times in the closed state. Therefore, it was necessary to restrict the analysis to conditions of voltage and $[Zn^{2+}]$ with well-resolved openings. In practice, most of the analyzed records exhibited an open-state lifetime ≥ 10 ms. Given a cutoff limit of 1 ms for the shortest detectible opening at 200-Hz filtering, this allows us to estimate the maximum fraction of missed openings as $1 - \exp(-1\text{ ms}/10\text{ ms}) = 0.1$.

Even though the open-state lifetime was generally well resolved, the measured lifetime is actually slightly longer than the true lifetime because openings are artificially lengthened by missed brief closures that are shorter than the dead time cutoff limit of 1–2 ms. Since the open-time histograms were monoexponential and the closed-time histograms approximated a sum-of-two exponentials with one predominant short component, it was reasonable in this case

to apply a simple correction to the fitted open-state lifetime that strictly applies to a case of monoexponential closed and open states where only brief closing events are missed (Colquhoun and Sigworth, 1983). The correction used was:

$$\tau_o = \tau_{o,obs} \exp(-T_d/\tau_C) \quad (1)$$

where τ_O is the corrected open-state lifetime, $\tau_{O,obs}$ is the open-state lifetime as observed by histogram fitting, T_d is the previously cited dead time, and τ_C is the fitted lifetime of the shortest fitted component in the closed-state histogram. Although Eq. 1 is not strictly applicable to our situation due to the presence of multiple components in the closed-state histogram, we believe that it is a safe method for normalizing the observed open times for variations in the lifetime of the short closed component that occur as Zn^{2+} concentration is increased (Fig. 10). Since the short component in the closed-state histogram lies in the range of 10–25 ms for most of the experiments (see Fig. 10), Eq. 1 gives a maximum correction of 10% on the observed open-state lifetime at low Zn^{2+} concentrations. Omitting this correction does not affect our major conclusion that the open-state lifetime is inversely proportional to $[Zn^{2+}]$ (Fig. 7 and 11 *A*).

In the absence of Zn^{2+} we observed that closed-state histograms typically exhibit a fast and slow component with respective lifetimes in the range of 1–3 ms and 100–300 ms (e.g., Fig. 9 *A*). The slow component consists of well-resolved closures, but the fast component includes many incomplete closings due to the detection limit of 1–2 ms. The addition of Zn^{2+} results in the appearance of a new intermediate lifetime in the range of 15–25 ms that includes the large majority of all observed closing events. After the addition of Zn^{2+} the slow 100–300-ms lifetime component due to gating closures was still present, but the fast 1–3-ms component appeared to be buried in the short lifetime edge of the Zn^{2+}-induced component. Since it is technically impossible to distinguish brief unresolved gating events from brief closures due to the substate events, we fitted the closed-state populations in the presence of Zn^{2+} with two exponentials and assumed that the fast component is a valid approximation of the substate population. This assumption appears to be justified since inspection of the actual records indicates that the number of substate events observed in the presence of Zn^{2+} greatly outnumbers brief closures in the absence of Zn^{2+} (see Fig. 1).

A second consideration in measuring the duration of brief substate closures in the presence of Zn^{2+} by using a single discriminator set at a 50% threshold is the possibility of transitions between the substate level and the fully closed state. Possible examples of such transitions are shown in the record of Fig. 4 at −70 mV, where it appears that there are several examples of transitions between the current levels labeled c and s1. This particular record was filtered at 50 Hz for the purpose of obtaining well-resolved amplitude histograms. At 200-Hz filtering, preferred for dwell-time analysis, the increased noise superimposed on the c and s1 levels actually prevents the reliable discrimination of real transitions between s1 and c from false transitions due to baseline noise. Thus, under the filtering conditions of our kinetic study we cannot easily quantitate the impact of this problem on measurements of substate duration. However, inspection of long records with many substate events suggests that the large majority of closures to the s1 substate level are not contaminated by s1-closed-s1 or s1-closed-open transitions. If such events were common, we would expect to observe excess noise in the region of the s1 and c current levels during the long bursts of Zn^{2+}-induced flickers in comparison to the baseline noise of the closed state. Examination of Figs. 1, 2, and 3 indicates that such excess noise is not present. We have recently been able to conduct a more rigorous examination of this question by studying the Zn^{2+}-induced substate phenomenon at higher permeant ion concentrations of 1.0 and 2.0 M NaCl. Under these conditions the s1 substate current is markedly increased and we are able to clearly resolve and quantitate the various types of transitions between the open, s1, and closed levels. Our preliminary results indicate that transitions between the closed and s1 levels in the presence of Zn^{2+} occur at a frequency that is $<2\%$ of the

primary open-s1-open transitions, which are the object of study in this paper. This supports our assumption here, that the 50% threshold method for measuring substate durations is not seriously compromised by the presence of transitions between the closed and s1 levels.

A final consideration in the measurement of substate durations is the artificial lengthening of such events that occurs due to missed brief openings. As mentioned previously, we purposely restricted our analysis to conditions of voltage and Zn^{2+} concentrations where the observed open-state dwell time is >10 ms, or ~ 5–10 times greater than the dead time. Despite this precaution, this phenomenon could affect our conclusion that the s1 substate duration increases as a function of Zn^{2+} concentration, since the number of missed openings would be expected to increase with increasing Zn^{2+}. This effect could result in an overestimation of the true substate duration as Zn^{2+} increases. To estimate the magnitude of this effect we calculated the worst case correction of the closed time expected for a two-state model under the conditions of our analysis. These estimates were made using theoretical corrections for a two-state model given by Milne et al. (1989), where the same dead time applies to missed brief closures and missed brief openings. In Fig. 10 this exercise indicated that the observed substate duration is at most 20% greater than the true substate duration for data points in Fig. 10 in the range of 40–80 μM Zn^{2+}. As discussed in Results, it appears that the magnitude of this effect cannot fully account for the observed observed lengthening of the apparent substate duration with increasing [Zn^{2+}] in the range of 10–80 μM.

RESULTS

Single Na^+ Channel Currents in the Presence of External Zn^{2+} Exhibit a Complex Pattern of Activity

Fig. 1 illustrates the single-channel behavior of a BTX-modified, cardiac Na^+ channel before (control) and after the addition of 20 μM Zn^{2+} to the extracellular side of the channel. In the absence of Zn^{2+} such BTX-modified Na^+ channels exhibit a high open-state probability, P_o, in the voltage range more positive than −70 mV: P_o = 0.77 ± 0.10 at −70 mV and P_o = 0.93 ± 0.05 at +70 mV (±SD, n = 8 channels). As shown in Fig. 1 at −50 mV, control records exhibit two types of closing events in the absence of Zn^{2+}: short closures (*a*) that are often incompletely resolved due to the limited time response and long closures (*b*) of 50–1,000-ms duration that close completely to the zero current level. This pattern of activity suggests a two-exponential distribution of closed-state events that is described later in more detail (Fig. 9 *A*). In control records, substate transitions defined by well-resolved events at intermediate current levels are quite infrequent. However, in the absence of Zn^{2+} we have occasionally observed examples of substate transitions near the open state that close to ~90% of the open-current level (not shown).

The addition of 20 μM Zn^{2+} to the extracellular side of the channel induces the immediate appearance of rapidly flickering behavior. This effect is fully reversible as can be demonstrated by the addition of sufficient EDTA to chelate free Zn^{2+} (not shown). The lower 1-min recording in Fig. 1 is marked to illustrate a variety of phenomena observed in the presence of Zn^{2+}. Long bursts (*c*) of flickering activity can be discerned that are separated by long b-type closures similar to those in the control record. Within the flickering burst there are many brief (<100 ms) Zn^{2+}-induced closures (*d*) to a new s1 subconductance level that is shown in Fig. 4 at higher gain. Fig. 1 also shows two examples of another type of rare substate event (*e*) induced by

Zn^{2+} which resides at a distinctly higher current level than the s1 level of d-type closures.

This complex pattern of single-channel activity in the presence of Zn^{2+} includes transitions between at least four distinct current levels. A complete description of the kinetic behavior of such systems is not readily amenable to detailed analysis because of the large number of states and transitions that must be involved. To simplify the problem, in this paper we focus on a description of a specific subset of the behavior shown in Fig. 1. This subset involves the primary type of transitions between the fully

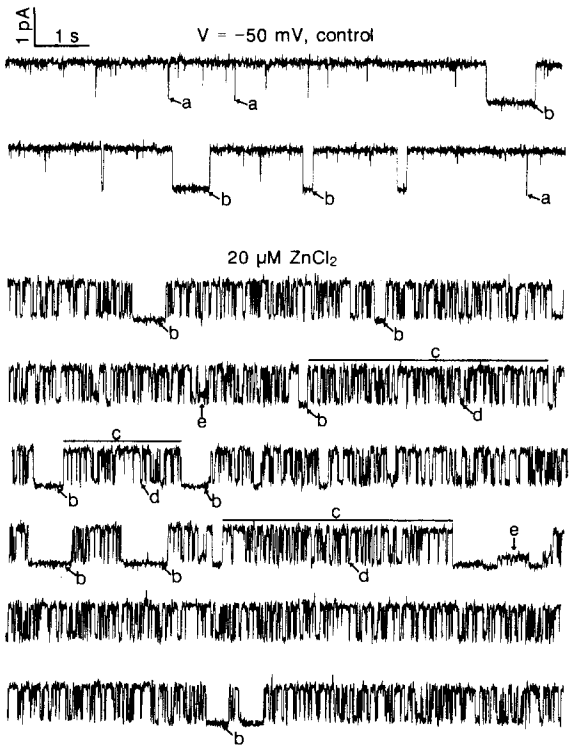

FIGURE 1. Current records of a single cardiac Na^+ channel in the absence and presence of external Zn^{2+}. The top two traces are continuous 10.2-s records of a BTX-modified cardiac Na^+ channel recorded at −50 mV in the presence of symmetrical 0.2 M NaCl, 10 mM MOPS-NaOH, pH 7.4. The recording is filtered at 100 Hz and channel opening is upward. The top control record illustrates examples of two types of closing events discussed in text: *a*, short closures; *b*, long closures. The bottom six traces are a continuous record from the same control channel taken after addition of 20 μM $ZnCl_2$ to the external chamber. This record illustrates various types of behavior observed in the presence of Zn^{2+}: *b*, long closures to the zero current level similar to those in the control trace; *c*, burst of Zn^{2+}-induced flickering events; *d*, brief (<100 ms) Zn^{2+}-induced closures to a subconductance level; *e*, examples of a second rare type of substate level induced by Zn^{2+} with higher conductance than that of d-type closures.

open state and the predominant s1 substate denoted by the d-type events in Fig. 1. To extract and analyze the kinetics of this particular subset of events from the record, we make certain assumptions regarding the ability of our sampling technique to select fairly pure populations of dwell times corresponding to s1-open-s1 and open-s1-open transitions. These assumptions are justified in more detail in Methods.

Fig. 2 (−70 mV) and Fig. 3 (+70 mV) show expanded 1-s records of the Zn^{2+} substate behavior from a different bilayer recorded in the presence of increasing concentrations of external Zn^{2+}. The records of Figs. 2 and 3 are both oriented with

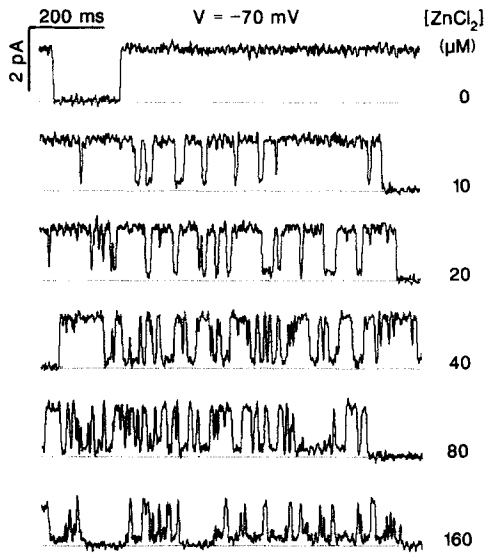

FIGURE 2. Concentration dependence of Zn^{2+}-induced substate events in a single cardiac Na^+ channel prolonged by BTX. The horizontal line at the bottom of each trace is drawn through the closed or zero current level determined by complete closures such as those shown in the top control record in the absence of Zn^{2+}. Conditions: symmetrical 0.2 M NaCl, 10 mM MOPS-NaOH, pH 7.4, and external Zn^{2+} concentrations ranging from 10 to 160 μM as indicated. The holding voltage was −70 mV throughout. 100-Hz filtering.

upward openings to facilitate direct comparison of the Zn^{2+}-induced blocking events. The top traces of Figs. 2 and 3 in the absence of Zn^{2+} show segments of the recording containing a b-type closing event with a duration of ~200 ms. Such resolved closings can be used to unambiguously identify the closed-current level, defined as zero current and marked with a dotted line in each trace. These expanded records show that external Zn^{2+} produces brief substate closures that have an average duration of ~20 ms. This experiment also shows that the frequency of the Zn^{2+}-induced blocking events increases with Zn^{2+} concentration. Aside from closure to a substate, this behavior resembles other cases of discrete block of ion channels by inorganic cations

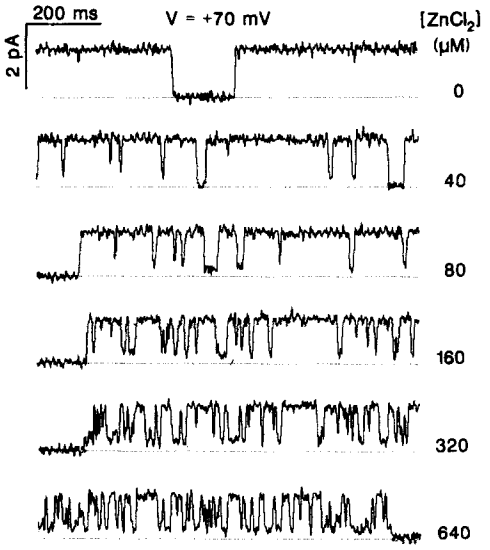

FIGURE 3. Concentration dependence of Zn^{2+}-induced substate events at +70 mV. The same channel studied in the experiment of Fig. 2 at −70 mV is shown here at +70 mV to illustrate the voltage dependence of Zn^{2+}-induced fluctuations. Note the higher external Zn^{2+} concentrations (40–640 μM) as compared with Fig. 2. The zero current level (closed) is marked with a horizontal line in each trace.

such as Ba^{2+} block of large conductance Ca^{2+}-activated K^+ channels (Vergara and Latorre, 1983) or Cd^{2+} block of Ba^{2+} current through L-type Ca^{2+} channels (Lansman et al., 1986). Comparison of Figs. 2 and 3 also shows that the relative duration of the Zn^{2+} blocking events is not strongly voltage dependent; however, the frequency of the Zn^{2+}-induced events is voltage dependent. About a 10-fold higher concentration of Zn^{2+} is required to produce the same number of blocking events per second at +70 mV vs. −70 mV. By analogy to other examples of discrete block at a single site, this behavior is suggestive of a voltage-dependent association rate for Zn^{2+} and a voltage-independent dissociation rate.

Current–Voltage Behavior of the Major Substate Induced by Zn^{2+}

When current records of Zn^{2+}-induced substates are closely examined as a function of voltage, it appears that the substate current is slightly larger at positive holding

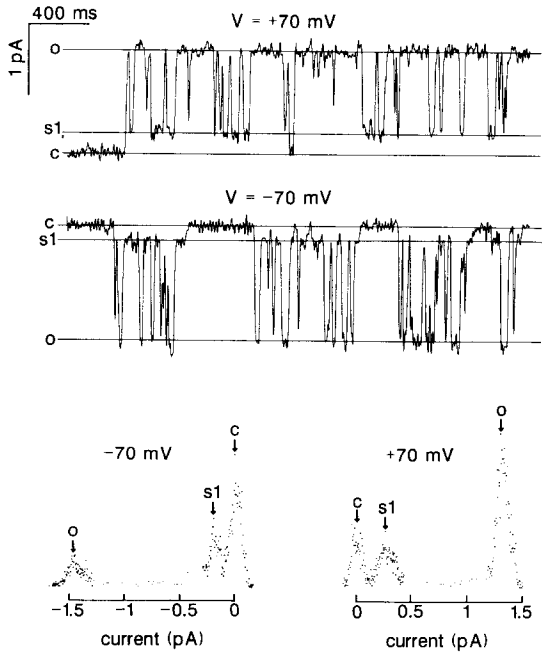

FIGURE 4. Resolution of Zn^{2+}-induced substate current by amplitude histograms. The upper two traces are portions of current records of the same channel (50-Hz filtering) taken at holding potentials of +70 mV in the presence of 80 μM Zn^{2+} and −70 mV in the presence of 20 μM Zn^{2+}. The amplitude histograms shown at the bottom were compiled from the upper records as described in Methods. Current levels are identified as closed (*c*), open (*o*), and Zn^{2+}-induced substate (*s1*). Ordinate scales in the histograms correspond to 89 points/bin for the peak value of the closed state at −70 mV and 81 points/bin for the peak value of the open state at +70 mV.

voltages compared with negative holding voltages. Th is is illustrated in Fig. 4, where enlarged current traces of subconductance events are shown at −70 and +70 mV along with corresponding amplitude histograms. In Fig. 4 the current level of the resolved substate is marked by a horizontal line labeled s1 drawn by eye through the mean noise level of the longest duration substate events. Comparison of the substate current relative to the open (*o*) and closed (*c*) current levels in Fig. 4 indicates that the s1 substate is 13% of the open-channel current at −70 mV and 22% of the open-channel current at +70 mV. This slight asymmetry of the substate current is

verified by the positions of current peaks in the amplitude histograms of Fig. 4 and the *I-V* relationships for the open state and the s1 substate presented in Fig. 5.

As described previously for BTX-modified Na^+ channels from other sources (Moczydlowski et al., 1984*a*; Hartshorne et al., 1985; Green et al., 1987; Recio-Pinto et al., 1987; Behrens et al., 1989), the *I-V* curve of the open state of the cardiac Na^+ channel approximates a linear relation in the presence of symmetrical NaCl. This ohmic behavior measured in the voltage range of −70 to +100 mV corresponds to a slope conductance of 21 pS. For the s1 substate we calculate a slope conductance of 3.1 pS or 15% of open-channel current for negative holding voltages (−50 to −100 mV) and 5.1 pS or 25% of open-channel current for positive holding voltages (+50 to +100 mV). These results indicate that the *I-V* relation of the s1 substate is outwardly rectifying with an approximate rectification ratio of 1.6 for outward current to inward current (Fig. 5).

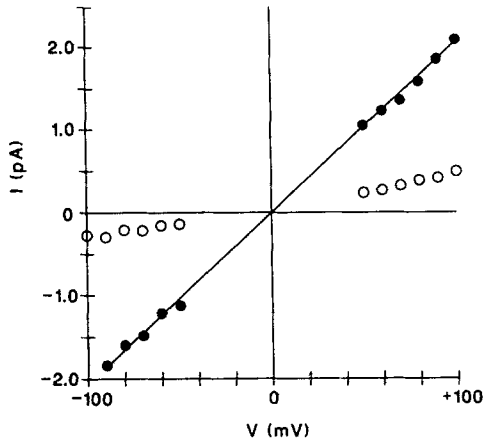

FIGURE 5. Current–voltage behavior of the open state and the Zn^{2+}-induced substate. Unitary currents of the open state (●) and the substate (○) were measured using amplitude histograms as illustrated in Fig. 4 or by direct measurements on expanded records with a mouse-driven cursor. The linear fit to the data for the open state is described by a slope conductance of 21 pS. Data points indicate the mean of measurements pooled from five different channels. Standard errors are smaller than the symbols.

Consideration of a Simple Blocking Model for Substate Production by Zn^{2+}

As noted above, the concentration dependence of the substate events illustrated in Figs. 2 and 3 is qualitatively similar to that observed in other cases of discrete block of single channels by ligands that bind in a reversible fashion, except that Zn^{2+} induces a substate. To determine whether the kinetics of the primary substate behavior corresponds to a reversible binding process, the following model was considered:

$$\begin{array}{ccc} O + Zn & \underset{k_{off}}{\overset{k_{on}[Zn]}{\rightleftharpoons}} & S{\cdot}Zn \\ \alpha \downarrow & & \\ C & & \end{array}$$

(Scheme 1)

Scheme 1 implies that binding of Zn^{2+} to a single site on the open channel, O, results in a substate form of the channel complexed with Zn^{2+}, S·Zn. By analogy to the case of reversible discrete block at a single site (Colquhoun and Hawkes, 1983), this

scheme predicts that dwell-time histograms of the open state and Zn^{2+}-blocked substate will exhibit single exponential distributions with time constants, τ_o for the open state and τ_s for the substate, which are respectively given by:

$$\tau_o^{-1} = k_{on}[Zn] + \alpha \quad (2)$$

$$\tau_s^{-1} = k_{off} \quad (3)$$

These relationships indicate that the time constant for the open state is inversely

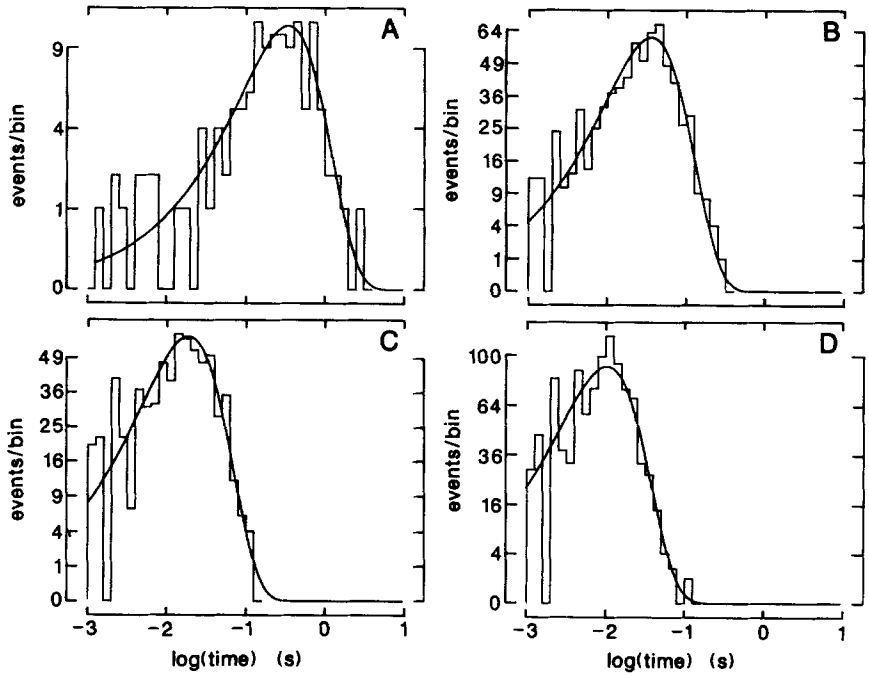

FIGURE 6. Frequency density histograms of open-state dwell times. Dwell-time populations of open state events at −70 mV for the same channel in the absence of Zn^{2+} (*A*) and in the presence of Zn^{2+} (*B*, 10 μM Zn^{2+}; *C*, 20 μM; *D*, 40 μM) were compiled and analyzed as described in Methods. The Sigworth-Sine histogram representation using a square root scale for the ordinate and a log-binned abscissa is shown (Sigworth and Sine, 1987). Solid lines are single exponential fits with time constants as follows: (*A*) control in the absence of Zn^{2+}, τ_o = 340 ms, n = 128 events; (*B*) 10 μM Zn^{2+}, τ_o = 35.6 ms, n = 700; (*C*) 20 μM Zn^{2+}, τ_o = 18.8 ms, n = 665; (*D*) 40 μM Zn^{2+}, τ_o = 10.3 ms, n = 995.

proportional to Zn^{2+} concentration and the time constant for the substate is independent of Zn^{2+} concentration.

As described in Methods, dwell-time histograms for open-state events and closed- or substate events were constructed using a simple 50% threshold criterion to identify the two classes of events at high or low conductance levels. Fig. 6 shows frequency density histograms of open-state durations compiled from 1-min segments of single-channel data recorded at −70 mV in the presence of 0, 10, 20, or 40 μM

external Zn^{2+}. Under all conditions we observed that such open-state histograms are well described by single exponential distributions. In the absence of Zn^{2+}, the cardiac Na^+ channel exhibited an apparent open-state lifetime of ~300 ms at −70 mV (mean = 315 ± 31 ms, ±SE, n = 11 channels) and 700 ms at +70 mV (mean = 737 ± 159 ms, n = 10). The weak voltage dependence of the open-state lifetime in the absence of Zn^{2+} is due to an increasing frequency of channel gating events at negative voltages, which is especially evident as the activation gating range (−80 to −120 mV) is approached. As external Zn^{2+} is increased, the observed open state lifetime progressively decreases. This is illustrated in Fig. 6 by the lifetime shortening from 35.6 ms at 10 μM Zn^{2+} (Fig. 6 *B*) to 18.8 ms at 20 μM Zn^{2+} (Fig. 6 *C*) and 10.3 ms at 40 μM Zn^{2+} (Fig. 6 *D*).

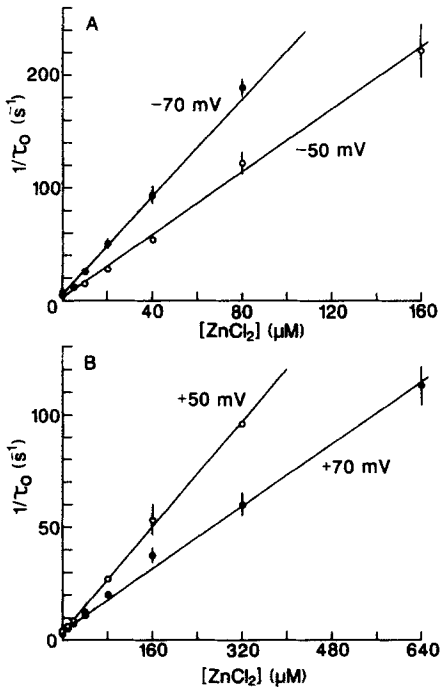

FIGURE 7. Linear relationship between reciprocal open-state lifetime and Zn^{2+} concentration. The open-state lifetime in the presence of various Zn^{2+} concentrations was determined by fitting open-state, dwell-time populations to a single exponential as shown in Fig. 5 and corrected according to Eq. 1 in Methods. The reciprocal of the corrected lifetime is fit to a linear function of $[Zn^{2+}]$ according to Eq. 2 for data obtained at negative voltages of −70 and −50 mV (*A*) or positive voltages of +50 and +70 mV (*B*). Error bars indicate ±SD for 8–10 different bilayers.

As discussed in Methods, the open-state lifetimes measured by the histograms in Fig. 6 are apparent lifetimes, overestimated by the limitation of detecting very short closing or blocking events. By applying a small correction described in Methods, such apparent open-state lifetimes can be corrected so that they more accurately reflect a true open-state lifetime. The reciprocal of such corrected open-state lifetimes measured at ±50 and ±70 mV is plotted as a function of Zn^{2+} concentration in Fig. 7. This figure illustrates our general finding that these two parameters are linearly related. At very high Zn^{2+} the open-state lifetimes become shorter than we can accurately measure (<5 ms). Thus our analysis is generally restricted to a range of Zn^{2+} where τ_o > 10 ms.

Eq. 2 also predicts a non-zero ordinate intercept of τ_0^{-1} vs. $[Zn^{2+}]$, which is due to a Zn^{2+}-independent pathway of closing from the open state included in Scheme 1. If this closing step is described by a rate constant, α, linear regression analysis indicates that α is essentially independent of voltage in the range of ± 70 mV with a mean value of $\alpha = 3.6 \pm 0.4\ s^{-1}$ ($\pm$SE, for determinations at eight different voltages).

According to Eq. 2, the slope of plots of τ_o^{-1} vs. $[Zn^{2+}]$ corresponds to k_{on}, a bimolecular association rate constant for Zn^{2+}. The results of Fig. 7 show that this rate constant increases with hyperpolarization in a voltage-dependent fashion. In Fig. 8 *A* k_{on} is plotted according to the following exponential function of voltage:

$$k_{on}(V) = k_{on}(0) \exp(-z_{on}'FV/RT) \quad (4)$$

where $k_{on}(0)$ is the Zn^{2+} association rate at 0 mV, $RT/F = 25.4$ mV at 22°C, and z'_{on} is

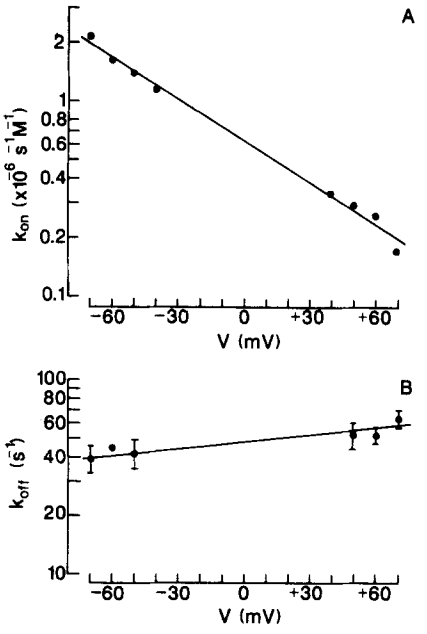

FIGURE 8. Voltage dependence of apparent association rate constant and dissociation rate constant for Zn^{2+}, assuming the simple blocking model of Scheme 1. (*A*) k_{on} as determined from the slope of plots of τ_o^{-1} vs. $[Zn^{2+}]$ (e.g., Fig. 7). (*B*) k_{off} as determined from the mean value of $\tau_{c,fast}^{-1}$ at Zn^{2+} concentrations ≥ 40 μM (e.g., Fig. 10). Fits of the data to exponential functions of voltage (Eqs. 4 and 5) are given in the text.

a slope parameter. From a linear fit of the logarithm of k_{on} vs. voltage, we obtain $k_{on}(0) = 6.3 \times 10^5\ s^{-1}M^{-1}$ and $z'_{on} = 0.42$. This latter value for the voltage slope parameter of the association reaction is similar to that previously estimated from analysis of the equilibrium probability of opening vs. $[Zn^{2+}]$ ($z' = 0.42$–0.47, Ravindran et al., 1991). Within the framework of Scheme 1, this comparison suggests that most of the voltage dependence for the Zn^{2+}-blocking reaction lies in the Zn^{2+} association step.

In contrast to the frequency density histograms for the open state, interpretation of the closed-state histograms is complicated by the presence of multiple components (Fig. 9). As discussed in Methods, technical considerations preclude the compilation of a pure population of substate events from single-channel records of the cardiac Na^+ channel under the present recording conditions. However, a unique component

associated with the primary Zn^{2+}-induced substate can be identified in the closed-state histograms.

Fig. 9 *A* shows a typical example of a closed-state histogram compiled from 1 min of a single-channel record in the absence of Zn^{2+}. At holding voltages more depolarized than the range for gating activation (> −80 mV), the sample of events obtained for 1 min of such control data is usually quite small (n = 128 in Fig. 8 *A*); however, it is clear that at least two exponential components are required to fit the

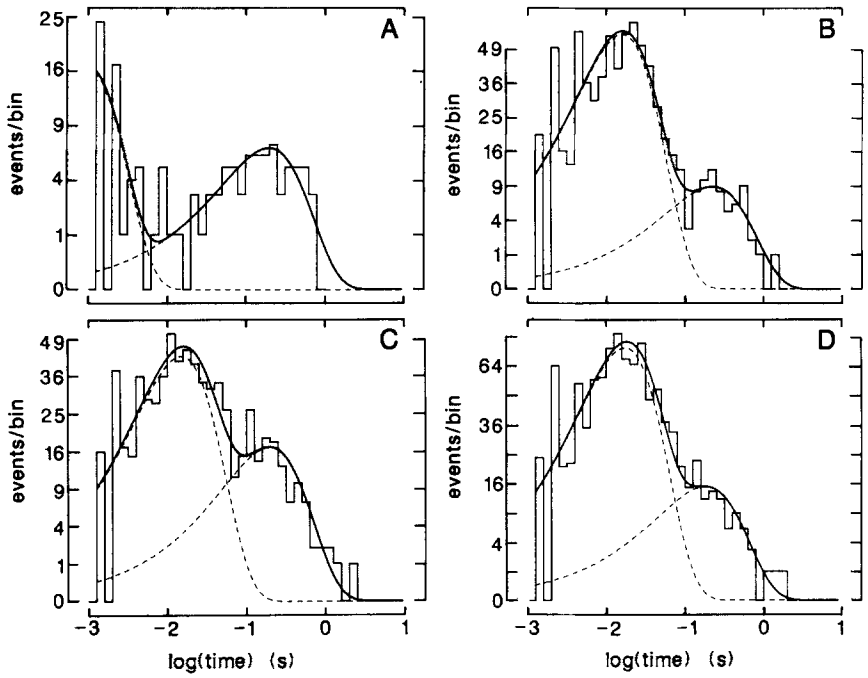

FIGURE 9. Frequency density histograms of closed-state dwell times in the absence and presence of Zn^{2+}. Dwell-time populations of closed-state events for a single channel at −70 mV were compiled and analyzed as described in Methods. Solid lines are a fit to a sum of two exponentials with the individual components shown by the dashed lines. (*A*) Control in the absence of Zn^{2+}, τ_{fast} = 0.90 ms, A_{fast} = 0.72, τ_{slow} = 198 ms, A_{slow} = 0.28, n = 128 events; (*B*) 10 μM Zn^{2+}, τ_{fast} = 15.9 ms, A_{fast} = 0.86, τ_{slow} = 224 ms, A_{slow} = 0.14, n = 669; (*C*) 20 μM Zn^{2+}, τ_{fast} = 15.1 ms, A_{fast} = 0.72, τ_{slow} = 196 ms, A_{slow} = 0.28, n = 666; (*D*) 40 μM Zn^{2+}, τ_{fast} = 17.5 ms, A_{fast} = 0.83, τ_{slow} = 183 ms, A_{slow} = 0.17, n = 966.

observed distribution. This observation agrees with previous investigations of the gating kinetics of BTX-modified Na^+ channels from a variety of sources (Huang et al., 1984; French et al., 1986; Keller et al., 1986). Such studies have shown that single exponential distributions are usually sufficient to describe closed-state distributions within the gating range of −120 to −80 mV, but a sum-of-two exponentials is required at more positive voltages. In the example of Fig. 9 *A*, at −70 mV two lifetime components of 0.9 and 198 ms were fit to the distribution as indicated by the

theoretical curves. From these lifetime estimates it is apparent that the long component is composed of complete closures that are well resolved, such as the b-type closures in control records of Fig. 1. On the other hand, the short component contains a majority of events with dwell times <5 ms, which are incompletely resolved at our cutoff resolution limit of 1 ms.

Similar histograms accumulated in the presence of Zn^{2+} contain many more events and also require at least two exponential components for an adequate fit. Fig. 9, *B–D* presents closed-time histograms for the same channel taken in the presence of 10, 20, and 40 μM Zn^{2+}. Comparison of the fits in Fig. 9 indicates that the lifetime of the long component is invariably ~200 ms in the absence and presence of Zn^{2+}, but the short component exhibits a lifetime of 15–18 ms in the presence of Zn^{2+} (Figs. 9, *B–D*) as compared with 1 ms in the absence of Zn^{2+} (Fig. 9 *A*). The results of Fig. 9 at −70 mV exemplify a general observation that the Zn^{2+}-induced substate phenomenon is associated with a new component in the closed-state histogram with a lifetime of 10–25 ms. In some cases it appeared that closed-state histograms in the presence of Zn^{2+} were better described by a sum-of-three exponentials, with an additional component in the range of 1 ms. However, this very fast component was always poorly resolved and difficult to analyze in a quantitative fashion. Therefore, we routinely fit all closed-time histograms with two exponentials and considered the resulting fast component, $\tau_{c,fast}$, as a lifetime associated with the s1 substate process.

As further support for the exclusion of the slow component from the process of Zn^{2+} inhibition, we found that the lifetime of the slow component generally lies in the range of 100–500 ms from channel to channel and does not appear to be significantly affected by Zn^{2+} at voltages from −70 to +70 mV. We also found that the average amplitude of the long component in the presence of Zn^{2+} is ~0.1 at −70 mV and 0.03 at +70 mV (data not shown). Inspection of actual records such as those in Fig. 1 also reveals that most of the long duration closing events are complete closures rather than substate events. Thus, it appears that the lifetime of the short component, $\tau_{c,fast}$, measured in the presence of Zn^{2+}, reflects the actual duration of substate events. Consideration of a variety of possible sampling errors discussed in Methods suggests that $\tau_{c,fast}$ is a good estimate of the lifetime of s1 substate closures under the conditions we have selected.

In Fig. 10 the mean lifetime values of $\tau_{c,fast}$ averaged from three to eight bilayers are plotted as a function of $[Zn^{2+}]$ at six different holding voltages in the range of −70 to +70 mV. These results do not correspond to the predictions of Eq. 3 from Scheme 1, since this lifetime increases as a function of $[Zn^{2+}]$, particularly at low Zn^{2+}. However, at Zn^{2+} concentrations greater than 40 μM, $\tau_{c,fast}$ appears to saturate at values near 15 ms at −70 mV and 25 ms at +70 mV.

For the moment we will assume that the value of $\tau_{c,fast}$ at high Zn^{2+} provides an estimate of k_{off} according to Eq. 3. Such estimates of k_{off} from the reciprocal of $\tau_{c,fast}$ obtained in the range of 40–320 μM Zn^{2+} are plotted in Fig. 8 *B*, where k_{off} is described by the following exponential function of voltage analogous to Eq. 4:

$$k_{off}(V) = k_{off}(0) \exp (z_{off}'FV/RT) \quad (5)$$

From a fit of the k_{off} data to Eq. 5 we obtain $k_{off}(0) = 48.2\ s^{-1}$ and $z'_{off} = 0.06$. According to the model represented by Scheme 1 the relationships of Eqs. 4 and 5

should also predict the equilibrium behavior of Scheme 1 by a voltage-dependent equilibrium dissociation constant for Zn^{2+} binding, $K_d(V) = k_{off}(V)/k_{on}(V)$, or

$$K_d(V) = K_d(0) \exp(z'FV/RT) \quad (6)$$

Taking the ratio of Eqs. 5 and 4 using the previously derived parameters, $k_{on}(0)$, $k_{off}(0)$, z'_{on}, and z'_{off}, we obtain $K_d(0) = 77$ μM and $z' = 0.48$. Despite the anomalous behavior of $\tau_{c,fast}$ at low Zn^{2+}, these values compare rather favorably to those previously estimated from an analysis of Zn^{2+} titrations of the equilibrium open-state probability of the heart channel: $K_d(0) = 58$–67 μM; $z' = 0.42$–0.47 (Ravindran et al., 1991). This agreement between the kinetic and equilibrium behavior suggests that Scheme 1 is an adequate model of Zn^{2+} inhibition in the range where the substate duration is essentially independent of Zn^{2+}; i.e., at >40 μM Zn^{2+}.

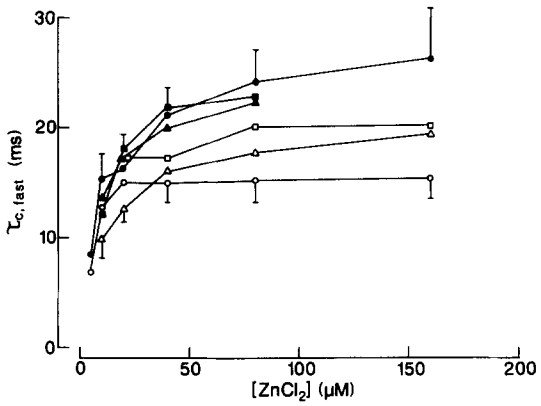

FIGURE 10. Dependence of the fast time constant of the closed state on Zn^{2+} concentration. Event populations of dwell-time histograms for the closed state were fit to a sum of two exponentials as illustrated in Fig. 9. Mean values of the fast time constant determined at various voltages are plotted as a function of [Zn^{2+}] (●, −70 mV; ■, −60 mV; ▲, −50 mV; △, +50 mV; □, +60 mV; ○, +70 mV). Data points indicate the mean of measurements from three to eight different bilayers. Only selected error bars (±SE) are shown for the sake of clarity.

Consideration of a Conformational Model for Zn^{2+}-induced Substates

As discussed in Methods, the striking increase of the s1 substate duration measured by $\tau_{c,fast}$ in the range of 5–80 μM Zn^{2+} (Fig. 10) does not appear to be accounted for by errors that could result in overestimation of the substate duration. This observation indicates that the one-step blocking model of Scheme 1 is not a valid model of the substate process, especially at low Zn^{2+} concentrations. Therefore, we have considered a simple conformational model that can account for this kinetic behavior. Our interest in this model is heightened by the striking similarity between Zn^{2+}-induced substates of the cardiac Na^+ channel and the H^+- or D^+-induced substates observed for monovalent ion currents through L-type Ca^{2+} channels (Prod'hom et al., 1987; Pietrobon et al., 1989). In their analysis, Pietrobon et al. (1989) also observed that the apparent lifetime of H^+-induced substates increased as a function of H^+ concentration rather than being independent of concentration. From this observation they concluded that the lifetime of the substate does not strictly represent the residence time of a bound proton, but instead corresponds to the lifetime of a

substate conformation of the channel that also occurs in an unliganded state. According to such a conformational model, the process of Zn^{2+}-induced substate behavior minimally includes the following states:

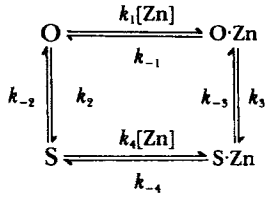

(Scheme 2)

In Scheme 2, O and S represent, respectively, fully open and s1 subconductance conformations of the channel which can interconvert with their respective Zn^{2+}-liganded forms, O·Zn and S·Zn. Scheme 2 can also be recognized as a form of the allosteric model of ligand-induced conformational change originally proposed by Monod et al. (1965).

As previously discussed by Pietrobon et al. (1989), this model actually predicts a two-exponential distribution for dwell-time histograms of both open and sublevel events. However, these authors also showed that only one exponential is observable because the other exhibits an insignificant amplitude over most of the accessible pH range and is also too brief to measure. Thus, rapidly interconverting conformational schemes, such as Scheme 2, can give rise to apparent single-exponential behavior.

To analyze the Zn^{2+} blocking kinetics using Scheme 2, we derived the reciprocal mean lifetime, τ_o^{-1}, of the grouped open state (O and O · Zn) and the reciprocal mean lifetime, τ_s^{-1} of the grouped sublevel states (S and S · Zn) from Eq. 74 in Colquhoun and Hawkes (1977). These predicted reciprocal mean lifetimes in terms of rate and equilibrium constants of Scheme 2 are:

$$\tau_o^{-1} = (k_2K_1 + k_3[\mathrm{Zn}])/(K_1 + [\mathrm{Zn}]) \tag{7}$$

$$\tau_S^{-1} = (k_{-2}K_4 + k_{-3}[\mathrm{Zn}])/(K_4 + [\mathrm{Zn}]) \tag{8}$$

In these equations, K_1 and K_4 are equilibrium dissociation constants for Zn^{2+} binding to the O and S conformations, respectively ($K_1 = k_{-1}/k_1$; $K_4 = k_4/k_4$). From the behavior of Eq. 7 in the limits of zero and infinite Zn^{2+}, the ordinate intercept of a plot of τ_o^{-1} vs. [Zn^{2+}] is equal to k_2 and τ_o^{-1} approaches an asymptote of k_3 at high [Zn^{2+}]. Comparison of these theoretical results with the data in Fig. 7 indicates that $k_2 \ll k_3$, since there is no saturation of τ_o^{-1} in the observable range. A similar analysis of the behavior of Eq. 8 in the limits of zero and infinite [Zn^{2+}], and comparison with the data of Fig. 9, indicates that $k_{-3} < k_{-2}$. From the requirement of microscopic reversibility of Scheme 2, we also have: $K_4/K_1 = K_3/K_2$, where $K_3 = k_{-3}/k_3$ and $K_2 = k_{-2}/k_2$. These relationships therefore imply that $K_4 \ll K_1$; i.e, Zn^{2+} binds with higher affinity to the substate conformation of the channel (S) than the open-state conformation (O). This analysis indicates that binding of Zn^{2+} to the O state greatly enhances the rate of conversion of the open state to the S·Zn conformation, thus effectively stabilizing or trapping the substate.

In an attempt to fit the observed kinetic behavior to Scheme 2, we first fit the dependence of τ_o^{-1} on $[Zn^{2+}]$ according to Eq. 7. Inspection of Fig. 7 indicates that the ordinate intercept, k_2, is well defined and apparently voltage independent in the range of −70 to +70 mV. We assumed a value of $k_2 = 3.6\ s^{-1}$, as obtained from the mean k_2 intercept at different holding voltages. From the apparent voltage independence of k_2 we assumed that the analogous k_3 reaction would also be voltage independent. The data of Fig. 7 at −70 and +70 mV were fit by theoretical curves with trial values of k_3 increasing from 300 s^{-1} and corresponding best-fit values of K_1. In fitting the τ_o data we observed that low values of k_3 produce too much curvature and the K_1 dissociation constant becomes unreasonably high at very large values of k_3. Since we are not sure of a realistic upper limit for k_3, the chosen value was kept as small as possible for an acceptable fit. We settled on $k_3 = 10^4\ s^{-1}$ for the Zn^{2+} block, which may be compared with the value of $k_3 = 2 \times 10^5\ s^{-1}$ used by Pietrobon et al. (1989), in modeling the faster H^+ block. Fig. 11 *A* shows the final fit to Eq. 7 based on τ_o data obtained at −70 and +70 mV with kinetic constants listed in Table I.

Next the dependence of τ_s^{-1} on $[Zn^{2+}]$ at −70 and +70 mV was fit using Eq. 8 and our measurements of $\tau_{c,fast}$ as estimates of τ_s. Inspection of Fig. 10 indicates that the k_{-3} plateau values are close to $k_{-3} = 40\ s^{-1}$ at −70 mV and $k_{-3} = 55\ s^{-1}$ at +70 mV. If k_{-2} is chosen as a variable in Eq. 8, the value of K_4 is constrained by the microscopic reversibility relationship, $K_1K_3 = K_2K_4$. As in our choice of k_3, we chose the smallest values of k_{-2} that resulted in a reasonable simulation of the τ_s data. Microscopic reversibility also requires that k_{-2} have the same voltage dependence as k_{-3}. By this approach we were able to simulate the saturating behavior of τ_s with respect to increasing $[Zn^{2+}]$ as shown in Fig. 11 *B*, but we were not able to accurately fit our observed data at low Zn^{2+}. Given the rather large standard errors of $\tau_{c,fast}$ due to experimental variation, the poor fits to Eq. 8 at low Zn^{2+} may be due to technical problems rather than a failure of the model to fit the data.

As a final step in our evaluation of Scheme 2 we compared the predicted open-state probability with results from the equilibrium titration of open-state probability for Zn^{2+} block at ±70 mV measured in the companion paper (Ravindran et al., 1991). Fig. 8 *B* of the preceding paper describes the probability of being unblocked ($P_{unblocked}$) in the presence of Zn^{2+}, which was computed as the ratio of the unconditional open-state probability in the presence of Zn^{2+} to that measured in the absence of Zn^{2+}. Since this parameter is normalized for the ~10–20% probability of channel closing in the absence of Zn^{2+}, it may be directly compared with the open-state probability of Scheme 2, which does not include closed states.

According to Scheme 2, the observed equilibrium open-state probability, P_{open}, equals the following ratio of the individual probabilities for each of the four states:

$$P_{open} = (P_O + P_{O\cdot Zn})/(P_O + P_{O\cdot Zn} + P_S + P_{S\cdot Zn}) \quad (9)$$

where $P_O + P_{O\cdot Zn} + P_S + P_{S\cdot Zn} = 1.0$. Eq. 9 can be used to derive the following expression for P_{open} in terms of the equilibrium constants of Scheme 2:

$$P_{open} = K_3(K_1 + [Zn])/[(K_4 + K_1K_3) + (1 + K_3)[Zn]] \quad (10)$$

Fig. 11 *C* shows that the simulated behavior of Scheme 2 using Eq. 10 and the equilibrium constants listed in Table I exhibit reasonable agreement with titration data for $P_{unblocked}$ taken from the preceding paper (Ravindran et al., 1991).

Although Scheme 2 is a simple kinetic framework that can be used to simulate the Zn^{2+}-induced substate process, we must stress that it is a minimal model that greatly underestimates the actual kinetic complexity. Scheme 2 does not include closed states

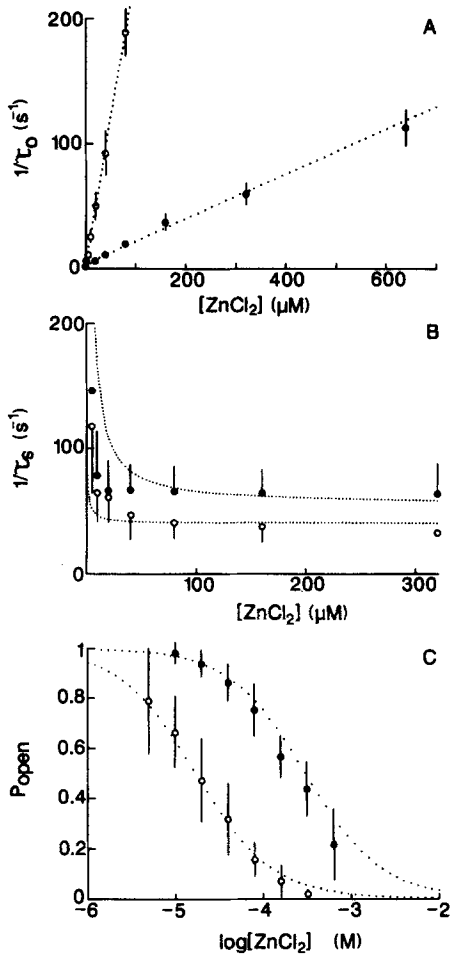

FIGURE 11. Simulation of the kinetic and equilibrium behavior of Zn^{2+}-induced substates with a four-state conformational model. (*A*) Fit of open-state lifetimes to Eq. 7 derived from Scheme 2. (*B*) Fit of reciprocal lifetimes of the fast, closed component to Eq. 8. (*C*) Fit of the equilibrium probability of Zn^{2+} block to Eq. 10. Data points are taken from Fig. 7 of this paper (*A*), Fig. 10 of this paper (*B*), and Fig. 8 *B* of Ravindran et al. (1991) (*C*). The data points are mean ± SE at −70 mV (○) or +70 mV (●). Values for the various kinetic constants used in the dotted line simulations are listed in Table I.

because we only attempted to describe the behavior of the open state and the short component of closures corresponding to apparent substate dwell times. In principle, a closed state (C) and a closed state with bound Zn^{2+} (C · Zn) may interconvert with the four states of Scheme 2, resulting in a six-state model linked by nine reversible routes of interconversion. Since it is known that BTX-modified Na^+ channels in the absence of Zn^{2+} exhibit at least two closed states, even such a model including one

type of closed state would not be sufficient. Thus, more realistic kinetic models of single-channel behavior in the presence of Zn^{2+} are considerably more complex than either of the two kinetic schemes considered in this paper.

DISCUSSION

This paper documents a new example of a unique type of blocking behavior involving the production of discrete substates in unitary currents of ion channels. The first example of this phenomenon was described by Prod'hom et al. (1987), who showed that protons and deuterium ions induce a substate level at 34% of the open-state current in L-type Ca^{2+} channels studied with Na^+ as the charge carrier. These authors initially suggested that this effect was mediated by a direct influence of an external negative charge on Na^+ permeation. They envisioned an ionizable site near the mouth of the channel that could directly affect the local concentration of permeant ions. At high pH the site would not be protonated and the channel would exhibit a high conductance. At low pH, with H^+ bound to the site, the net removal of a

TABLE I

Kinetic Constants Used for the Simulation of Scheme 2

Parameter	$V = -70$ mV	$V = +70$ mV
K_1	4.2×10^{-5} M	5.5×10^{-2} M
K_2	2×10^{3}	2.8×10^{3}
K_3	4×10^{-5}	5.5×10^{-3}
K_4	8.3×10^{-9} M	1.1×10^{-7} M
k_{-2}	7.3×10^{3} s^{-1}	1×10^{4} s^{-1}
k_2	3.6 s^{-1}	3.6 s^{-1}
k_{-3}	40 s^{-1}	55 s^{-1}
k_3	1.0×10^{4} s^{-1}	1.0×10^{4} s^{-1}

The tabulated values were used to simulate the kinetic behavior of Scheme 2 using Eqs. 7–9. Results of the simulation are shown as dotted theoretical curves in Fig. 11.

negative charge would result in a lower Na^+ concentration near the mouth of the channel and a subconductance state.

However, further mechanistic studies and tests of this model (Pietrobon et al., 1988, 1989; Prod'hom et al., 1989) led to its abandonment in favor of a conformational model involving a structural transition of the channel from a high conductance form to a low conductance form mediated by binding of H^+ to a site distant from the pore. Some of the evidence cited for this new model included: voltage independence of the kinetics of H^+-induced fluctuations between -70 and -120 mV, dependence of the apparent deprotonation rate constant on the concentration and species (Na^+, K^+, Cs^+) of the permeant ion, lack of direct binding competition between H^+ and an occluding blocker (Ca^{2+}), and an increase in the duration of substate dwell times with increasing H^+ concentration. The apparent complexity of such behavior cannot readily be accounted for by a simple effect on a negative charge at the mouth of the channel. In particular, to interpret the interaction between permeant ions and H^+

binding, allosteric coupling between the H^+ binding site and site(s) for permeant ions in the conduction pathway was invoked.

Although mechanistic analysis of Zn^{2+}-induced substate behavior in cardiac Na^+ channels is at an early stage, our present results suggest that a simple model based on a one-step Zn^{2+} binding reaction (Scheme 1) is also inadequate. Our study of dwell-time distributions of the substate suggest that substate durations increase as a function of Zn^{2+} concentration (Fig. 10), which is not predicted by the one-step dissociation process of a direct blocking mechanism (Scheme 1). In additional experiments at higher NaCl concentrations and better resolution we find that this latter behavior is a consistent finding (Schild, L., A. Ravindran, and E. Moczydlowski, unpublished observations). As previously discussed by Pietrobon et al. (1989) for H^+-induced substate behavior, this observation requires inclusion of a substate conformation of the unliganded channel in any successful kinetic model of substate fluctuations. Therefore, even if the Zn^{2+} (or H^+) binding site is located near the outer mouth of the channel, conformational changes must be invoked in addition to any direct effect on Na^+ permeation.

Students of ion channel blocking mechanisms realize that it is difficult to prove an intrapore location of a blocking ion in the absence of direct structural information. On this basis it is even more difficult to prove that an ion-binding site is located near the mouth of a channel from functional studies alone, because allosteric models can usually be proposed that will predict similar behavior. For example, the fact that we observe $z\delta = 0.46$ for the Zn^{2+} substate behavior does not necessarily require that the Zn^{2+} binding site is located at an electrical distance of 0.23 within the electric field traversing the pore. Previous studies have documented examples of voltage-dependent binding where the voltage dependence is not directly correlated with the charge(s) of the blocking species (Moczydlowski et al., 1984*b*). In such cases, the voltage dependence of binding may arise via indirect conformational coupling with regions of the protein that directly respond to voltage. Perhaps the most convincing evidence for block by physical interference or occlusion is supplied by cases where the blocking ion can produce the inhibitory effect from both sides of the channel, so that the blocker is actually shown to permeate at a low rate. For example, Ba^{2+} block of large conductance Ca^{2+}-activated K^+ channels exhibits such signs of direct permeation expected of an intrapore blocker (Neyton and Miller, 1988). In the case of H^+-induced substates of L-type Ca^{2+} channels, Prod'hom et al. (1989) showed that the substate effect does not occur at low internal pH, implying that the H^+-binding site cannot be reached by protons passing through the channel from the inside. Similarly, we have also found that concentrations of external Zn^{2+} that produce an effective substate block of cardiac Na^+ channels are ineffective when added to the internal side of the channel (Ravindran, A., and E. Moczydlowski, unpublished results). While additional experiments are required before a partial occlusion model of substate block by Zn^{2+} can be eliminated, our present experience suggests that this phenomenon does not easily fit into the category of occluding blocker mechanisms.

Another example of substate block in a different ion channel was reported in a study of the effect of Cs^+ and Rb^+ on inward rectifying K^+ channels in isolated heart cells (Matsuda et al., 1989). In this case, the blocking pattern exhibited two equally spaced subconductance levels. Analysis of this behavior using the binomial theorem

was consistent with a model involving three equivalent conducting pathways independently blocked by Cs^+ or Rb^+; i.e., a triple-barreled channel. The effect of Zn^{2+} on heart Na^+ channels that we have identified appears to be quite distinct from this type of behavior. Although there are at least two distinct sublevels induced by Zn^{2+}, the most frequent s1 level and a higher conductance substate shown in Fig. 1, the Zn^{2+}-induced substates do not occur as simple integer fractions of the open-state current and do not exhibit a binomial pattern characteristic of independent subunits. Thus, it seems unlikely that the Zn^{2+}-induced substates reflect any particular multibarreled structure of heart Na^+ channels.

The more obvious similarity between the characteristics of Zn^{2+}-induced substates in cardiac Na^+ channels and H^+-induced substates in L-type Ca^{2+} channels could well be related to an underlying structural homology of these two classes of voltage-sensitive channels. Cloning studies of neuronal, muscle, and cardiac subtypes of Na^+ channels and the muscle receptor for dihydropyridine Ca^{2+} channel blockers have revealed strong homologies in the primary sequence of these pseudotetrameric proteins (Tanabe et al., 1987; Rogart et al., 1989; Trimmer and Agnew, 1989). Based on this structural similarity between known Na^+ channel subtypes and the probable channel-forming subunit of a Ca^{2+} channel, we suggest that the Zn^{2+} binding site responsible for substate block in the cardiac Na^+ channel may be structurally analogous to similar H^+ binding sites(s) in the L-type Ca^{2+} channel.

One possible difference between Zn^{2+} block of the cardiac Na^+ channel and H^+ block of Ca^{2+} channels concerns the voltage dependence of these two phenomena, since Prod'hom et al. (1989) showed that the kinetics of the H^+-induced fluctuations are independent of voltage in the range of -120 to -70 mV. However, we note that these authors observed almost no H^+-induced substate behavior for outward currents at $+80$ mV and an external pH of 7.4, compared with strong substate block of inward currents under the same pH conditions at -80 mV (Fig. 2, Prod'hom et al., 1989). This latter observation does suggest relief of H^+ block at high positive voltages and may indicate voltage- or current-dependent behavior in this voltage range. Comparative studies of the mechanism of Zn^{2+}- and H^+-induced substate production in the two types of voltage-dependent ion channels may identify other common features that underlie the conformational changes responsible for these blocking behaviors. Even if the H^+ block of the Ca^{2+} channel and Zn^{2+} block of Na^+ channels do not occur at structurally analogous sites, other common structural elements that stabilize substate conformations of the two types of channels could be involved. For example, if one or more of the interface regions of contact between the four pseudosubunits become destabilized after Zn^{2+} or H^+ binding, such contact regions could collapse to form a tighter oligomeric structure with a smaller pore diameter, resulting in a transient substate.

An important prediction of the conformational model of Zn^{2+}-induced substates (Scheme 2) is that the Na^+ channel is expected to exhibit a low frequency of substate production in the absence of Zn^{2+}. Although we have not directly observed such Zn^{2+}-independent substate events that coincide with s1-type events, such substates in the absence of Zn^{2+} may be too brief to detect with the time resolution attainable in planar bilayers. It is possible that the fast component observed in dwell-time

histograms of closing events in the absence of Zn^{2+} contains a certain number of such unresolved substate closings. With patch clamp recording of normal and drug-treated Na^+ channels from mouse skeletal muscle, Patlak (1988) has observed brief subconductance events in the absence of Zn^{2+} with an amplitude of 35% of the open-state current. Since the amplitude of these substates is similar to that of the Zn^{2+}-induced substates that we observe, this observation provides support for the basic predictions of a model such as Scheme 2, which involves Zn^{2+}-dependent and -independent substate conformations.

In studies of a different class of voltage-dependent ion channels, our laboratory recently discovered another example of ligand-induced substate behavior. In this case we found that toxin I, a member of the peptide family of snake dendrotoxins, induces long-lived ($\tau = 40$ s) substate events when added to the internal side of large conductance Ca^{2+}-activated K^+ channels from rat skeletal muscle (Lucchesi and Moczydlowski, 1990). The mechanism of this toxin-induced substate phenomenon appears to involve conversion of the channel from a conformation with ohmic current–voltage behavior to a lower conductance conformation with inwardly rectifying current–voltage behavior. Given the various examples of substate behavior discussed above, conformational changes induced by ligand-binding that result in altered energy profiles for ion permeation may reflect a common aspect of channel function.

Summary

How do divalent cations inhibit the permeation of monovalent cations through ion channels? Before our investigation of this question in muscle and cardiac Na^+ channels, there was evidence for two types of mechanisms involving either direct occlusion of the channel or indirect screening of negative surface potential. The apparent voltage dependence of blocking ions was considered to be a manifestation of the direct influence of the transmembrane electric field on ion binding. Our observation of Zn^{2+}-induced substates in heart Na^+ channels and the apparent inadequacy of a one-step blocking reaction for this behavior is suggestive of a third kind of inhibitory mechanism analogous to the effect of protons in L-type Ca^{2+} channels. Our initial results suggest that the Zn^{2+}-induced substate represents a conformational change affecting ion permeation. The finding of voltage-dependent substate production has two implications for future models of channel function. One implication concerns the interpretation of "fast block" behavior manifested as a lower unitary conductance caused by various types of inorganic and organic blocking ions. Our results suggest that the microscopic basis for this behavior may sometimes include the production of transient substates in addition to complete transitions to the closed current level. A second implication concerns models of ion permeation. Our results imply that the complete energy profile of open channels consists of a dynamic equilibrium of multiple substates.

We thank Dr. John Daly for the gift of batrachotoxin.

This work was supported by grants from the National Institutes of Health (AR-38796 and HL-38156), the Searle Scholars Program/Chicago Community Trust and an Established Investigator award to E.

Moczydlowski from the American Heart Association, and a fellowship to L. Schild from the Swiss National Science Foundation.

Original version received 31 August 1989 and accepted version received 30 July 1990.

REFERENCES

Baumgarten, C. M., and H. A. Fozzard. 1989. Cd^{2+} and Zn^{2+} block unitary Na^+ currents in Purkinje and ventricular cells. *Biophysical Journal.* 55:313*a*. (Abstr.)

Behrens, M. I., A. Oberhauser, F. Benzanilla, and R. Latorre. 1989. Batrachotoxin-modified sodium channels from squid optic nerve in planar bilayers. Ion conduction and gating properties. *Journal of General Physiology.* 93:23–41.

Blatz, A. L., and K. L. Magleby. 1986. Correcting single channel data for missed events. *Biophysical Journal.* 49:967–980.

Colquhoun, D., and A. G. Hawkes. 1977. Relaxation and fluctuations of membrane currents that flow through drug-operated channels. *Proceedings of the Royal Society of London B Biological Sciences.* 199:231–262.

Colquhoun, D., and A. G. Hawkes. 1983. The principles of the stochastic interpretation of ion-channel mechanisms. *In* Single Channel Recording. B. Sakmann and E. Neher, editors. Plenum Publishing Corp., New York. 135–175.

Colquhoun, D., and F. J. Sigworth. 1983. Fitting and statistical analysis of single-channel records. *In* Single Channel Recording. B. Sakmann and E. Neher, editors. Plenum Publishing Corp., New York. 191–263.

Frelin, C., C. Cognard, P. Vigne, and M. Lazdunski. 1986. Tetrodotoxin-sensitive and tetrodotoxin-resistant Na^+ channels differ in their sensitivity to Cd^{2+} and Zn^{2+}. *European Journal of Pharmacology.* 122:245–250.

French, R. J., J. F. Worley, M. B. Blaustein, W. O. Romine, K. K. Tam, and B. K. Krueger. 1986. Gating of batrachotoxin-activated sodium channels in lipid bilayers. *In* Ion Channel Reconstitution. C. Miller, editor. Plenum Publishing Corp., New York. 363–383.

Green, W. N., L. B. Weiss, and O. S. Andersen. 1987. Batrachotoxin-modified sodium channels in planar lipid bilayers. Ion permeation and block. *Journal of General Physiology.* 89:841–872.

Guo, X., A. Uehara, A. Ravindran, S. H. Bryant, S. Hall, and E. Moczydlowski. 1987. Kinetic basis for insensitivity to tetrodotoxin and saxitoxin in sodium channels of canine heart and denervated rat skeletal muscle. *Biochemistry.* 26:7546–7556.

Hartshorne, R. P., B. U. Keller, J. A. Talvenheimo, W. A. Catterall, and M. Montal. 1985. Functional reconstitution of the purified brain sodium channel in planar lipid bilayers. *Proceedings of the National Academy of Sciences, USA.* 82:240–244.

Huang, L. M., N. Moran, and G. Ehrenstein. 1984. Gating kinetics of batrachotoxin-modified sodium channels in neuroblastoma cells determined from single-channel measurements. *Biophysical Journal.* 45:313–322.

Keller, B. U., R. P. Hartshorne, J. A. Talvenheimo, W. A. Catterall, and M. Montal. 1986. Sodium channel in planar lipid bilayers. Channel gating kinetics of purified sodium channel modified by batrachotoxin. *Journal of General Physiology.* 88:1–23.

Lansman, J. B., P. Hess, and R. W. Tsien. 1986. Blockade of current through single calcium channels by Cd^{2+}, Mg^{2+}, and Ca^{2+}. Voltage and concentration dependence of calcium entry into the pore. *Journal of General Physiology.* 88:321–347.

Lucchesi, K., and E. Moczydlowski. 1990. Subconductance behavior in a maxi Ca^{2+}-activated K^+ channel induced by dendrotoxin-I. *Neuron.* 2:141–148.

Matsuda, H., H. Matsuura, and A. Noma. 1989. Triple-barrel structure of inwardly-rectifying K^+ channels revealed by Cs^+ and Rb^+ block in guinea-pig heart cells. *Journal of Physiology.* 413:139–157.

Milne, R. K., G. F. Yeo, B. W. Madsen, and R. O. Edeson. 1989. Estimation of single channel kinetic parameters from data subject to limited time resolution. *Biophysical Journal.* 55:673–676.

Moczydlowski, E., S. S. Garber, and C. Miller. 1984*a*. Batrachotoxin-activated Na^+ channels in planar lipid bilayers. Competition of tetrodotoxin block by Na^+. *Journal of General Physiology.* 84:665–686.

Moczydlowski, E., S. Hall, S. S. Garber, G. R. Strichartz, and C. Miller. 1984*b*. Voltage-dependent blockade of muscle Na^+ channels by guanidinium toxins. Effect of toxin charge. *Journal of General Physiology.* 84:687–704.

Monod, J., J. Wyman, and J.-P. Changeux. 1965. On the nature of allosteric transitions. A plausible model. *Journal of Molecular Biology.* 12:88–118.

Neyton, J., and C. Miller. 1988. Potassium blocks barium permeation through a calcium-activated potassium channel. *Journal of General Physiology.* 92:549–567.

Patlak, J. B. 1988. Sodium channel subconductance levels measured with a new variance-mean analysis. *Journal of General Physiology.* 92:413–430.

Prod'hom, B., D. Pietrobon, and P. Hess. 1987. Direct measurement of proton transfer rates to a group controlling the dihydropyridine-sensitive Ca^{2+} channel. *Nature.* 329:243–246.

Prod'hom, B., D. Pietrobon, and P. Hess. 1989. Interactions of protons with single open L-type calcium channels. Location of protonation site and dependence of proton-induced current fluctuations on concentration and species of permeant ion. *Journal of General Physiology.* 94:23–42.

Pietrobon, D., B. Prod'hom, and P. Hess. 1988. Conformational changes associated with ion permeation in L-type calcium channels. *Nature.* 333:373–376.

Pietrobon, D., B. Prod'hom, and P. Hess. 1989. Interactions of protons with single open L-type calcium channels. pH dependence of proton-induced current fluctuations with Cs^+, K^+ and Na^+ as permeant ions. *Journal of General Physiology.* 94:1–21.

Ravindran, A., and E. G. Moczydlowski. 1988. Subtype-selective block of sodium channels by zinc studied at the single channel level in planar bilayers. *Abstracts of the Society of Neuroscience.* 14:835. (Abstr.)

Ravindran, A., L. Schild, and E. Moczydlowski. 1991. Divalent cation selectivity for external block of voltage-dependent Na^+ channels prolonged by batrachotoxin. Zn^{2+} induces discrete substates in cardiac Na^+ channels. *Journal of General Physiology.* 97:000–000.

Recio-Pinto, E., D. S. Duch, S. R. Levinson, and B. W. Urban. 1987. Purified and unpurified sodium channels from eel electroplax in planar lipid bilayers. *Journal of General Physiology.* 90:375–395.

Rogart, R. B., L. L. Cribs, L. K. Muglia, D. D. Kephart, and M. W. Kaiser. 1989. Molecular cloning of a putative tetrodotoxin-resistant rat heart Na^+ channel isoform. *Proceedings of the National Academy of Sciences, USA.* 86:8170–8174.

Roux, B., and R. Sauvé. 1985. A general solution to the time interval omission problem applied to single channel analysis. *Biophysical Journal.* 48:149–158.

Schild, L., A. Ravindran, and E. Moczydlowski. 1990. Zinc-induced subconductance events in cardiac sodium channels prolonged by batrachotoxin. *Biophysical Journal.* 57:297*a*. (Abstr.)

Sigworth, F., and S. Sine. 1987. Data transformation for improved display and fitting of single-channel dwell time histograms. *Biophysical Journal.* 52:1047–1054.

Tanabe, T., H. Takeshima, A. Mikami, V. Flockerzi, H. Takahashi, K. Kangawa, M. Kojima, H. Matsuo, T. Hirose, and S. Numa. 1987. Primary structure of the receptor for calcium channel blockers from skeletal muscle. *Nature.* 328:313–318.

Trimmer, J., and W. S. Agnew. 1989. Molecular diversity of voltage sensitive Na channels. *Annual Review of Physiology.* 51:401–418.

Vergara, C., and R. Latorre. 1983. Kinetics of Ca^{2+}-activated K^+ channels from rabbit muscle incorporated into planar lipid bilayers. Evidence for Ca^{2+} and Ba^{2+} blockage. *Journal of General Physiology.* 82:543–568.

Woodhull, A. M. 1973. Ionic blockage of sodium channels in nerve. *Journal of General Physiology.* 61:678–708.

Yamamoto, D., J. Z. Yeh, and T. Narahashi. 1984. Voltage-dependent calcium block of normal and tetramethrin-modified single sodium channels. *Biophysical Journal.* 45:337–344.